

Zeitschrift: IABSE reports = Rapports AIPC = IVBH Berichte
Band: 54 (1987)

Artikel: Large-scale analysis of gravity platforms
Autor: Arnesen, A. / Bergan, P.G. / Ottosen, N.S.
DOI: <https://doi.org/10.5169/seals-41943>

Nutzungsbedingungen

Die ETH-Bibliothek ist die Anbieterin der digitalisierten Zeitschriften. Sie besitzt keine Urheberrechte an den Zeitschriften und ist nicht verantwortlich für deren Inhalte. Die Rechte liegen in der Regel bei den Herausgebern beziehungsweise den externen Rechteinhabern. [Siehe Rechtliche Hinweise.](#)

Conditions d'utilisation

L'ETH Library est le fournisseur des revues numérisées. Elle ne détient aucun droit d'auteur sur les revues et n'est pas responsable de leur contenu. En règle générale, les droits sont détenus par les éditeurs ou les détenteurs de droits externes. [Voir Informations légales.](#)

Terms of use

The ETH Library is the provider of the digitised journals. It does not own any copyrights to the journals and is not responsible for their content. The rights usually lie with the publishers or the external rights holders. [See Legal notice.](#)

Download PDF: 12.05.2025

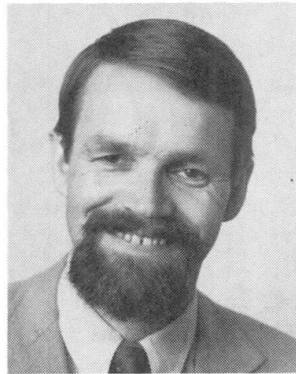
ETH-Bibliothek Zürich, E-Periodica, <https://www.e-periodica.ch>

Large-Scale Analysis of Gravity Platforms
Analyse des plates-formes de gravité
Berechnung von Betonplattformen grosser Abmessungen

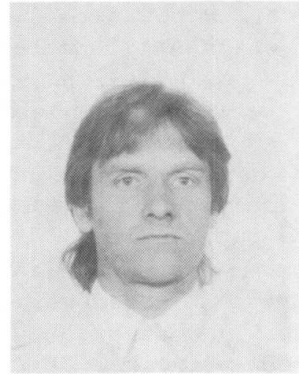
A. ARNESEN
Principal Res. Eng.
A.S. Veritas Research
Hoevik, Norway



P.G. BERGAN
President
A.S. Veritas Research
Hoevik, Norway



N.S. OTTOSEN
Assoc. Professor
Lund Inst. of
Techn.
Lund, Sweden



SUMMARY

The paper describes a coordinated effort to establish efficient and reliable methods and procedures for the analysis of large-scale gravity platforms placed in deep waters. Alternative concepts for concrete platforms and their characteristics are described. Constitutive models for inelastic behaviour of reinforced concrete are presented, and their applicability in connection with practical, large-scale analyses are discussed. Special emphasis is placed on realistic crack modelling of concrete. Finally, various computational aspects related to integrated, large-scale nonlinear static and dynamic finite element analyses are considered with particular reference to soil-structure interaction.

RÉSUMÉ

L'article décrit un effort coordonné pour établir des méthodes efficaces et sûres et des procédures pour l'analyse de grandes plates-formes de gravité, en eau profonde. D'autres concepts pour les plates-formes en béton et leurs caractéristiques sont décrits. Les modèles constitutifs du comportement inélastique du béton armé sont présentés et leurs applications, en relation avec des analyses pratiques et à large échelle, sont discutées. Une attention particulière est portée sur la modélisation réaliste des fissures du béton. L'article considère enfin différents aspects de calcul à l'ordinateur pour intégrer des études par éléments finis statiques et dynamiques tenant compte, en particulier, de l'interaction sol-structure.

ZUSAMMENFASSUNG

Der Beitrag beschreibt eine gemeinsame Anstrengung zur Erarbeitung von erfolgversprechenden und zuverlässigen Methoden und Berechnungsverfahren für grosse Schwergewichtsplattformen im tiefen Wasser. Alternative Konzepte für Betonplattformen und ihre charakteristischen Eigenschaften werden beschrieben. Materialgesetze für das unelastische Verhalten von Stahlbeton, ihre Anwendbarkeit auf Konstruktionen grosser Abmessungen und vor allem ein realistisches Rissmodell werden behandelt. Schliesslich werden verschiedene Berechnungsgesichtspunkte im Zusammenhang mit integrierten grossmassstäblichen nicht-linearen statischen und dynamischen Finite-Elemente-Analysen mit besonderer Berücksichtigung der Boden-Bauwerk-Interaktion behandelt.



1. INTRODUCTION

Up till now, about 20 concrete platforms for oil and gas production in the North Sea have been built or are under construction. The largest is the Gullfaks C platform, which is to be placed (1988) at 217 meters of water. However, concrete platforms for even deeper water are under planning, such as for the TROLL field, where the water depth is 300-350 meters. One of the proposed platforms for the Troll field, the T-300 platform, is 470 meters high, require 250,000 m³ of concrete, 60,000 tons of reinforcement and has a foundation area of 26,200 m². Completed and fully equipped it represents a value of approximately 3.5-4.0 billion USD. Description of some of these platforms may be found in [1,2,3].

Most of the previous concrete platforms have been designed on the basis of linear finite element analyses (with up to one million degrees of freedom) combined with cross-sectional checks against cracking and failure [4,5,6]. However, these procedures become insufficient as new platforms are to be placed in hostile waters with up to 350 meters depth, and in locations with very poor soil conditions where settlements could be more than 5 meters. Such situations calls for sophisticated design methods involving inelastic material modelling, and nonlinear static and dynamic finite element analyses, [7,8,9]. Considering the complexity of linear analysis of such structures it is evident that nonlinear analysis becomes quite a challenge. However, it is clear that a full-fledged nonlinear analysis of these problems cannot be carried out even with the most powerful computers available. The approach to be adopted must therefore be one of using nonlinear modelling where required and to combine this with simpler models elsewhere. Theoretical refinements and sophistication in the material modelling has to be weighed against what can be provided in terms of material parameters in practice. Reliability of a model is more important than sophistication per se.

The present paper addresses some of these problems in general terms and focuses on application to large-scale concrete platforms in particular.

2. DEEP WATER GRAVITY PLATFORMS

The experience from nearly 15 years with concrete oil production platforms in the North Sea has led to great confidence in this type of structures. Gravity platforms are kept in place by their own weight without piling and are hence the basis for their name. Typically, they consist of a multi-cylindrical, large volume caisson part which rests on the sea floor. From this three or more shafts extend beyond the water surface and support a steel deck on which the production equipment is placed, see Fig. 1. The caisson may serve as reservoir for storing oil, and the shafts may be used for drilling purposes as well as for production equipment. The slim shafts minimize the impact of the wave loading while the caissons and the large foundation area provide high structural stability.

Concrete platforms have a number of favourable features for offshore oil and gas production, such as; large deck areas on which heavy payloads can be accommodated, concrete minimizes costly inspection and maintenance work and they are well suited to sustain exhausting environmental conditions. These features become increasingly important as oil and gas production goes into deeper water. For the Troll field, the functional requirements have resulted in a need for a large platform in terms of oil production capacity, with an operational topside weight of 60,000 tons [10]. The environmental conditions at this field are extremely hostile with an estimated 100 years wave of 30.5 meters and with very poor soil conditions, consisting of very soft normal consolidated clay. This has great implications on the foundation design of the structure. The challenge posed by the soil are illustrated in Fig. 2, where the shear strength profile of the Troll field is compared with some other fields in the North Sea [11].

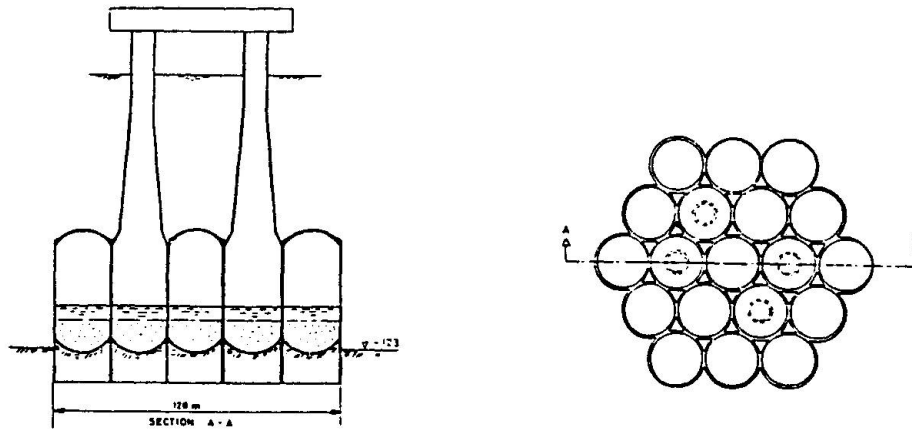


Fig. 1. Condeep concrete platform [3]

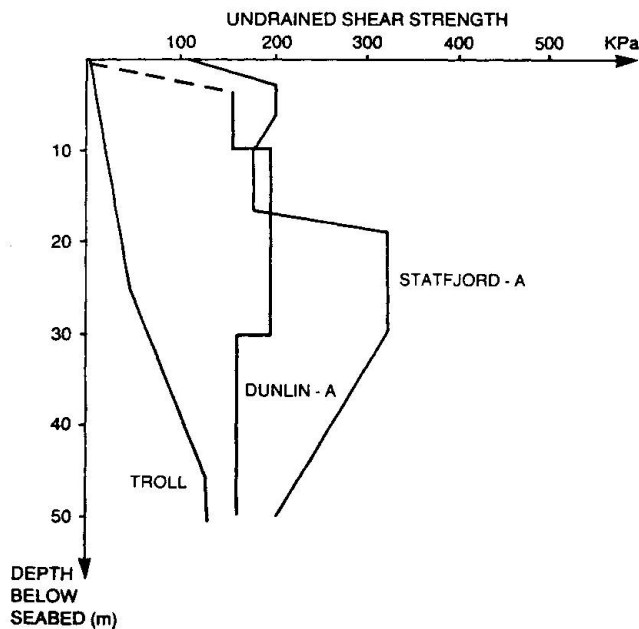


Fig. 2. Shear strength profiles of various fields in the North Sea [11]

The greatest uncertainties with respect to the soil problem lie in the determination of parameters in the response of the soil, to cyclic loading and in dynamic soil-structure interaction. The deep water and the soft supporting soil increase the dynamic effects of the wave loading. The loading effects are not only dependent upon the wave description and wave loading process alone, but also on the stiffness of the soil and damping of the structure-water-soil system. The fundamental period of deep water platforms may exceed the range of 4-6 seconds, approaching the typical period of high energy waves. This may in turn lead to significant dynamic amplification effects.

Soft soil conditions require special considerations in order to ensure sufficient safety against soil stability failure, to limit settlements and to assess the dynamic properties of the structure. Long skirts or piles underneath the platform penetrating into stiffer soil layers have been proposed for the Troll platform in order to give sufficient support for the structure. The long skirts, which may be of 20-30 meters length, are rather flexible; soil-structure interaction effects certainly have to be considered for the overall stiffness as well as for the dynamic response [13]. Nonlinear simulations are necessary in



order to verify various safety aspects of the soil-structure systems such as risk of failure, large inelastic deformation and progressive collapse. The design considerations involve extreme loading conditions due to wave loading, earthquake loading and accidental loads, combined with permanent loads and hydrostatic pressure loading of the submerged structure.

A variety of concrete platforms have been proposed for deep water; some of them are shown in Fig. 3. The Condeep SP and the Målfrid concepts shown in Figs. 3a and 3b, represent deep water versions of the commonly used Condeep concept, see Fig. 1. The T-300 and the Astrid platforms shown in Figs. 3c and 3d, are mono-shaft concepts especially designed for deep water installations. All of the concepts shown in Fig. 3 are equipped with long skirts underneath the platforms.

3. MODELLING OF REINFORCED CONCRETE

The complicated loading states and histories on deep water platforms, which include nonproportional loads, large hydrostatic pressure, as well as loading/unloading/reloading phenomena, place severe requirements on the constitutive models used. This implies that rather complicated constitutive models have to be resorted to in order to describe the inelastic behaviour and the extreme strength.

3.1 Failure criteria

The general constitutive models for concrete are normally based on the state of failure for concrete, i.e. the peak strength for a homogeneously loaded concrete specimen. Two alternative failure criteria expressed in terms of all three stress invariants are adopted in the present study; they are the Ottosen model [14] and the Willam-Warnke model [15]. A CEB report [16] as well as a state-of-the-art report by ASCE [17] support the choice of these models.

The failure criteria provide no indication of the type of failure, i.e. whether the failure is of the crushing (shearing) type or of the cracking type. Thus, an additional failure mode criterion has to be provided. It is assumed [18] that cracking occurs if the stress state violates the failure criterion in addition to that the maximum principal stress exceeds half the uniaxial tensile strength of the concrete. The crack plane is assumed to be normal to the direction of the maximum principal stress.

3.2 Tensile cracking

Accurate analysis of failure of concrete structures normally depends greatly on the modelling of the tension cracking process. Due to the discrete, localized nature of cracks, correct crack modelling is a difficult topic because it implies that discontinuities in the displacement field should be accounted for [19]. However, the extreme complexity of deep water platforms does not lend itself to discrete crack modelling, in fact, a total model would have to include millions of freedoms in order to account for discrete cracking in a satisfactory way. Instead, the smeared crack technique, originally proposed by Rashid [20], is adopted here.

In its original form, the smeared crack approach assumes the slope of the softening branch to be a material property. Special studies have demonstrated that this leads to the well known lack of objectivity [21]. Moreover, this original approach cannot model the structural size effect, which can easily be demonstrated experimentally for structures loaded primarily in tension [21,22].

In view of this, it is worth while focusing on the major improvements in crack modelling provided by the fictitious crack model [23] and the crack band model [24]. While the fictitious crack model is a two-parameter model (tensile strength, fracture energy), the crack band model is a three-parameter model (tensile strength, fracture energy, size of process zone). These models are able

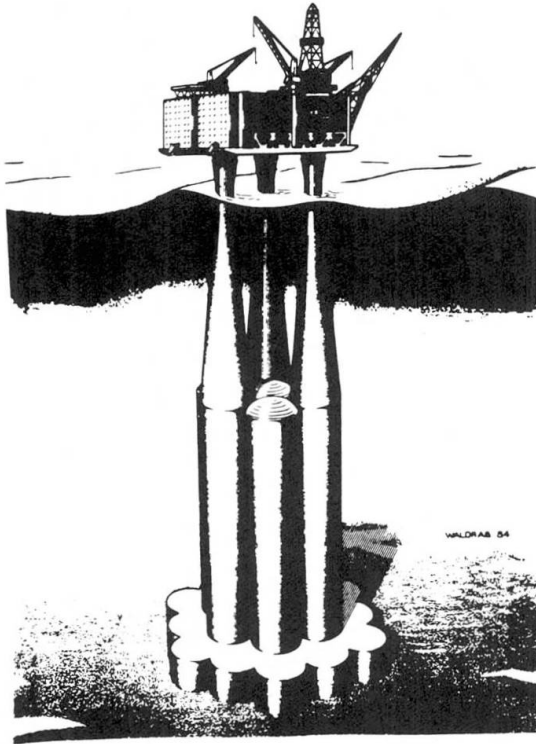


FIG. 3a CONDEEP SP3 [1]

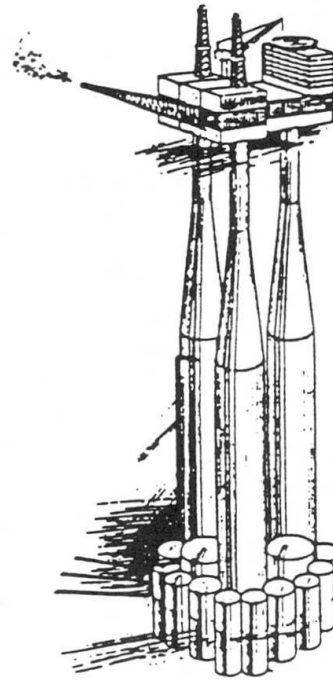


FIG. 3b MÅLFRID [2]

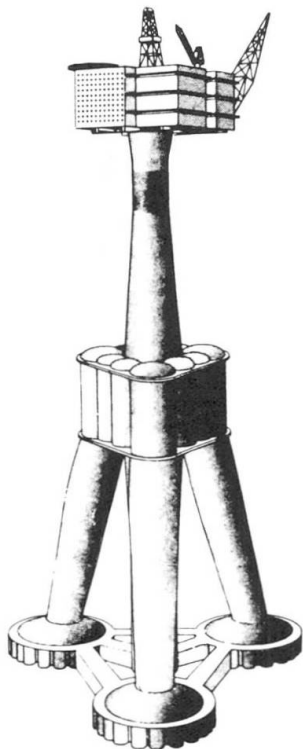


FIG. 3c T-300 [1]

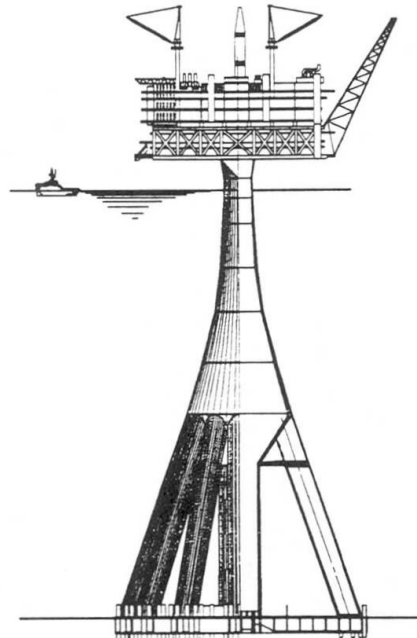


FIG. 3d ASTRID [12]

FIG. 3 Deep water concrete platforms



to describe all the essential phenomena related to crack modelling, but the use of these models in large-scale computer analyses raises some questions. In particular the crack band theory is directly applicable to a smeared cracking approach, and its use has been extensively verified for one particular type of element [24]. However, similar verifications for other element types are not yet available, in particular for cases in which the direction of cracking is not parallel to an element side. The fictitious crack model is in its original form a discrete approach, and, thus, it cannot be used for large-scale finite element calculations. A smeared version of the fictitious crack model was proposed in [25] for uniaxial elements and in [26,27,28] for general elements. In references [26,27,28], even the shear behaviour of smeared cracked elements was accounted for in a way similar to the fictitious crack model.

The present cracking procedure is based on the concept proposed in [26,27,28], in which the dissipated fracture energy, as well as the shear mechanism, is objective with respect to element mesh size and form.

The crack opening w^n normal to the plane of crack is assumed to be given by

$$w^n = (\sigma_t - \sigma)/N \quad \text{where } w^n > 0 \quad (1)$$

where σ_t is the uniaxial tensile strength, σ is the stress normal to the plane of crack and N is a material parameter. It can be shown that [26]

$$N = -E/\lambda \quad \text{where } \lambda = 2G_c E/\sigma_t^2 \quad (2)$$

where the material parameter λ is a characteristic length of the material and G_c is the fracture energy.

For a shear displacement, w^s , parallel to the plane of crack, the following simple relation is assumed

$$w^s = w^n \tau / G_s \quad (3)$$

where τ is the shear stress in the crack and G_s is the slip modulus which may be determined from experiments. A comparison between the simple form (3) and experimental data for $G_s = 3.8$ MPa shows very close agreement, see [27,28].

A key point to this crack formulation is the introduction of the so-called equivalent length, L_{eq} , which is a purely geometrical quantity dependent on the element mesh size and shape as well as the orientation of the crack. As an example, the definition of the equivalent length L_{eq} is illustrated in Fig. 4 for the constant strain triangle and the isoparametric 8-node membrane element with 2x2 Gauss point integration. It appears that L_{eq} is simply the maximum length internal of the element in the direction normal to the crack. In the case of isoparametric element the equivalent crack length is based on the subdomain belonging to the integration point considered, see Fig. 4.

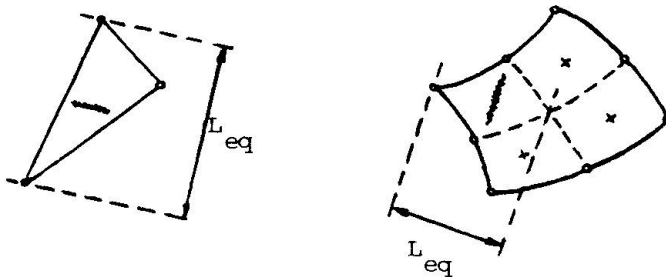


Fig. 4 Definition of equivalent length L_{eq}

For plane stress conditions the observations above lead to the following constitutive relation [26,27,28], where the x-axis is normal to the plane of the crack

$$\begin{bmatrix} \sigma_x \\ \sigma_y \\ \tau_{xy} \end{bmatrix} = \frac{E}{\alpha} \begin{bmatrix} 1 & \nu & 0 \\ \nu & 1 - \frac{\lambda}{L_{eq}} & 0 \\ 0 & 0 & \alpha \frac{G_{eff}}{E} \end{bmatrix} \begin{bmatrix} \epsilon_x \\ \epsilon_y \\ \gamma_{xy} \end{bmatrix} - \frac{\lambda}{\alpha} \frac{\sigma_t}{L_{eq}} \begin{bmatrix} 1 \\ \nu \\ 0 \end{bmatrix} \quad (4)$$

where

$$\alpha = 1 - \nu^2 - \frac{\lambda}{L_{eq}} \quad \text{where} \quad \lambda > L_{eq} \quad (5)$$

and the effective shear modulus, G_{eff} is given by

$$G_{eff} = \frac{G}{1 + \frac{G}{G_s} \frac{w^n}{L_{eq}}} \quad (6)$$

Note that G_{eff} is dependent on the crack opening, w^n , as well as on the equivalent length L_{eq} in such a way that G_{eff} decreases with increasing crack opening. It is seen that G_{eff} depends on the equivalent length in such a manner that the shear displacement of a cracked structure is independent on the size of the cracked element. This feature is of utmost importance and it has not been considered in previous crack models.

As an illustration of the application of this concept [27,28] consider the concrete specimen in Fig. 5 loaded by an increased elongation to complete separation. The following material parameters are assumed: $E = 2,1 \cdot 10^4$ MPa, $\nu = 0.2$, $\sigma_t = 3.3$ MPa, $G_s = 3.8$ MPa and $G_c = 130$ N/m

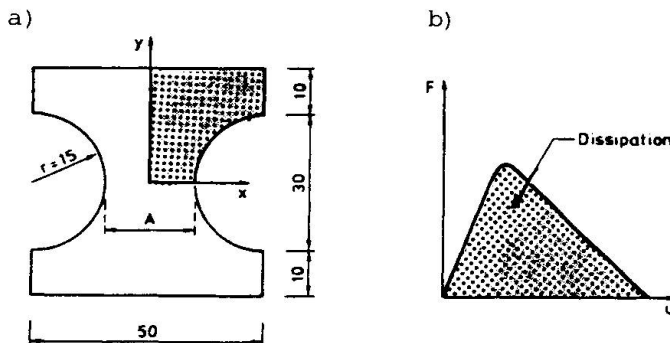


Fig. 5 Concrete tension specimen, A = cross sectional area

Due to symmetry, only one quarter of the tension specimen is considered. The purpose of the calculations is to verify that the adopted smeared crack approach is objective in the sense that the total cracking energy dissipated approaches the correct value. By definition, the total dissipated energy is AG_c , where G_c is the prescribed fracture energy per unit area $G_c = 130$ N/m and A is the cross sectional area of the specimen, see Fig. 5a. An outline of the total force - total elongation diagram is shown in Fig. 5b.

The specimen was analyzed using isoparametric 8-node elements with 2x2 Gauss integration points. The finite element meshes and the corresponding calculated force-elongation diagrams are shown in Fig. 6 and 7, respectively.

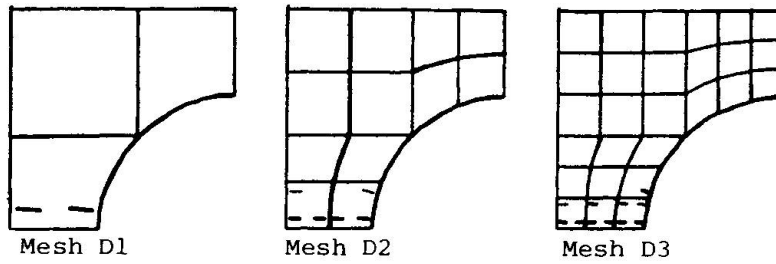


Fig. 6 Finite element meshes and crack patterns

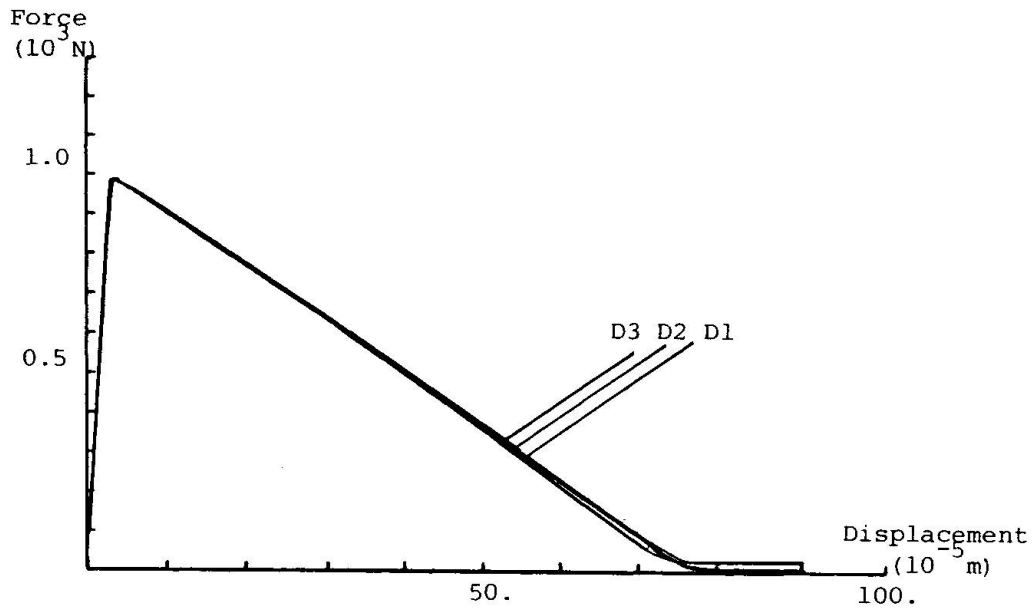


Fig. 7 Calculated force-displacement curves for meshes shown in Fig. 6

It appears from Fig. 7 that the result is almost independent of the element mesh size and; for the most detailed mesh, the calculated fracture energy is $G_{c,calc} = 129.1 \text{ N/m}$ as compared with the exact (input) value, $G_c = 130 \text{ N/m}$.

A more demanding situation is shown in Fig. 8 where the same type of element is tested for rather distorted meshes.

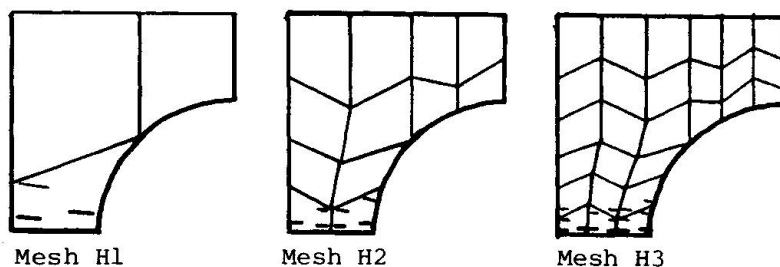


Fig. 8 Distorted finite element meshes and crack patterns

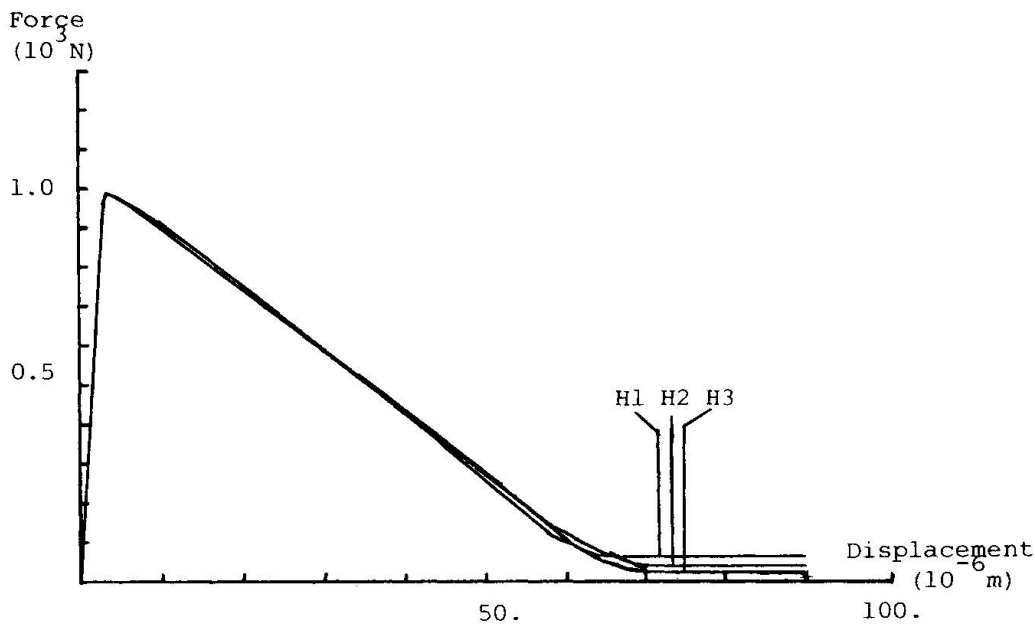


Fig. 9 Calculated force-displacement curves for meshes shown in Fig. 8

Fig. 9 shows the results to be almost independent of the element mesh size. For the most detailed mesh, the calculated fracture energy is $G_{c,calc} = 114.2$ N/m compared with the exact (input) value, $G_c = 130$ N/m. It is seen, however, that the force-displacement curves do not converge exactly to the zero value as they should. This is because of the distorted element meshes cannot reproduce the true crack pattern quite correctly, and hence shear stresses along the cracks contribute to a small load bearing capacity which is observed in Fig. 9.

3.3 Stress-strain models

The general three-dimensioned stress-strain behaviour of concrete is very complex, and it is characterized by effects like strain-hardening, strain-softening, dilatation, coupling effects between hydrostatic loading and deviatoric response and vice versa, elastic-plastic coupling and different behaviour in loading and unloading. It may therefore not be surprising that a general consensus does not exist as to the proper choice of stress-strain models applicable for general load paths. A wide range of constitutive models for concrete has been suggested in the literature, such as nonlinear elastic models, endochronic models, plastic-fracturing models and plasticity models.

Plasticity models are especially powerful, because realistic loading/unloading/reloading criteria may be formulated and the incremental stress-strain law may be derived directly. Moreover, the introduction of a yield surface makes plasticity models conceptually simple, as it becomes possible, a priori, to evaluate the qualitative behaviour of the models. The failure surface, which can be demonstrated experimentally, may be introduced explicitly in the model and utilized as yield surface.

The nonassociated plasticity model proposed by Han & Chen [29] is of particular interest. The yield surface is a closed surface in the stress space and, through a mixed kinematic-isotropic hardening formulation, the yield surface changes so that it becomes identical to the failure surface at peak-stresses. The yield potential surface is of the Drucker-Prager type. The model has been extensively verified by comparing its predictions with a wide range of stress histories including tensile loading as well as uniaxial, biaxial and triaxial compressive loadings. Also softening effects are accounted for. A main drawback of a nonassociated formulation is that the tangential stiffness matrix becomes non-symmetric.



3.4 Creep and shrinkage

Creep of concrete depends not only on the stress history, but also on the ageing of the concrete as well as on the histories of temperature and humidity. Hence, the determination of the time-dependent behaviour of concrete is a formidable task that calls for simplifications. Such simplifications should be in order for analysis of offshore structures as large creep strains are not expected due to the moderate temperatures and because the concrete is always rather old when exposed to the main loads. Moreover, as the mechanical loading mainly is caused by gravity and hydrostatic pressure, the stress changes over time are moderate.

The proportional relationship between creep strains and stresses is experimentally well established, as long as the sustained stress is below half the short-term strength for uniaxial compressive conditions. Moreover, Poisson's ratio under creep can be assumed to be equal to Poisson's ratio during short-term loading. These observations suggest that the so-called effective E-modulus method is sufficiently accurate for simulation of creep.

Shrinkage of concrete offshore platforms can normally be ignored for two reasons. First, these structures are composed of very massive and thick-walled concrete sections and, second, they are exposed to stable, humid conditions.

3.5 Reinforcement

The reinforcement has a completely different behaviour from concrete, and a separate treatment of the two materials and their interaction is necessary. A perfect bond between concrete and steel is assumed in this study, and for the representation of the reinforcement the so-called smeared concept [30] and embedded concept [31] are considered.

The smeared concept assumes that the reinforcement are uniformly distributed over the concrete element and the stiffness of the reinforcement is superimposed in a straightforward manner. The method is simple and it only requires a small amount of input data. Hence it is well suited for global analyses of concrete platforms when the overall behaviour of the structure is of main interest and no detailed information of stress distribution is required.

The smeared concept is not suited for dealing with inhomogenous reinforcement arrangement and arbitrary location of the bars within the concrete elements. The embedded concept, however, in which the reinforcement can be located arbitrarily within the concrete elements, has not such disadvantages. In localized analyses of sectional parts of the structure in which detailed information of the stress distribution, crack pattern, slip and bond failure is of primary interest, the embedded concept is superior to the smeared concept. The embedded concept implies, however, that the stiffness of each bar has to be determined in a straightforward, but rather cumbersome way. To avoid this problem, noting that a finite element model may include thousands of bars, an automatic search routine is under consideration. Knowing the end points of each bar or each layer of bars, the stiffness contribution may automatically be calculated using a geometrical search routine that determines the intersection between the bars and the concrete elements.

Only the axial stiffness of the bars need be considered and the stress-strain behaviour is modelled by a mixed kinematic-isotropic hardening rule. In this way reversed loadings due to dynamic excitation can be accounted for.

4. INTEGRATED SOIL-STRUCTURE ANALYSIS

The usual type of linear analysis of concrete offshore platforms involves two major idealizations with respect to soil-structure interaction: 1) the foundation of the structure is assumed to be rigid and 2) the skirts and the soil in between are assumed to be rigid. For deep water platforms equipped with flexible

skirts penetrating into very soft soil, however, it is necessary to account for the flexibility of the foundation, the skirts and the soil in between, for the evaluation of the dynamic response of the structure [32].

4.1 Dynamic soil-structure interaction analysis

Two main classes of methods are used for dynamic soil-structure interaction analysis: 1) frequency domain analysis and 2) time domain analysis [33]. The most common approach is frequency domain analyses which allows for the possibility of dividing the problem into substructures and introducing frequency dependent energy radiation at the boundaries. However, in order to account for nonlinear effects the solution has to be carried out in the time domain. Time domain soil-structure interaction methods may be categorized in three groups [34]; complete methods, boundary methods and volume methods.

The complete method assumes no superposition or substructuring and the problem is solved as a full-fledged nonlinear analysis. For soil-structure systems exhibiting extensive nonlinear behaviour this approach is necessary, however, costs and computer storage requirements related to such analyses normally limit the size of the problem that may be solved.

For earthquake analysis, the normal procedure is to divide the problem into a free field- or scattering problem and an interaction problem [33]. It is assumed that the total displacements of the soil consists of a free field contribution and an interaction contribution. In the free field analysis the excavated part of the soil may either be included (volume method) or excluded (boundary method). For nonlinear earthquake problems the boundary method is most suitable and is adopted here. The interaction contribution may account for nonlinearities in the structure and in the near field soil. This implies, however, that the excavation includes such a large part of the near field soil that the behaviour along the boundary of the excavation is predominately linear.

4.2 Modelling techniques

A full three dimensional model with solid finite elements is generally required to obtain satisfactory description of the nonlinear soil-structure problem. However, the nonlinearities in the soil will normally be confined to regions close to the structure and nonlinear material behaviour in the structure itself will normally be limited to critical sections in highly stressed areas. A significant reduction of the problem size may be obtained by limiting the nonlinear modelling to regions where substantial nonlinearities take place and by applying linear modelling elsewhere. Some techniques that may be utilized are:

1) Near field - far field modelling of the soil [34], see Fig. 10a. The near field, comprising regions of nonlinear behaviour, is modelled with solid elements. At a distance from the structure where the soil behaviour is linear and tends to behave like an axisymmetric system with nonaxisymmetric loads, the far field can be modelled by means of harmonic expansions of axisymmetric finite elements. At the interface, the displacements of the solid elements are expanded in Fourier series in order to match the corresponding displacement field of the axisymmetric elements.

2) Dynamic substructuring, see Fig. 10b. Dynamic substructuring implies that the total system is partitioned into linear and nonlinear regions and thereafter the number of degrees of freedom are reduced. Applying conventional implicit time integration schemes, the dynamic equilibrium equation can be replaced by an equivalent quasi-static incremental equilibrium expression [35] leading to an effective stiffness matrix and an effective load vector. A linear system, in which the effective stiffness matrix will be constant, lends itself to use of static condensation techniques, while a full nonlinear analysis implies that all terms have to be updated during the calculation.



3) Ritz-functions. Reduction of the number of freedoms may also be obtained by applying the concepts of component mode synthesis [33]. The displacements in the linear region are assumed to be constructed for a set of Ritz-vectors. This is done by considering the linear region fixed at the boundaries while the motion in the interior is described by a selected set of Ritz-vectors. This is combined with the overall solution for the nonlinear regions. A crucial point is the selection of Ritz vectors. To obtain reliable results these should be determined with due consideration of the inertia forces associated with the internal degrees of freedom. An alternative procedure is to use some of the lowest eigenvectors, however, this requires a significantly higher computational effort. Lanczos vectors may also be used.

4) Combination of solid elements and beam elements. Linear and moderate nonlinear regions of the structure may be represented by beam elements while regions with extensive nonlinearities (cracking, crushing and yielding of the concrete and reinforcement) are represented by nonlinear solid elements. This may be a viable approach when detailed knowledge of stress distribution in the beam element regions is not required. The global loads and the corresponding deformation state of the structure will in this way be accounted for in the solid element solution of the localized nonlinear regions.

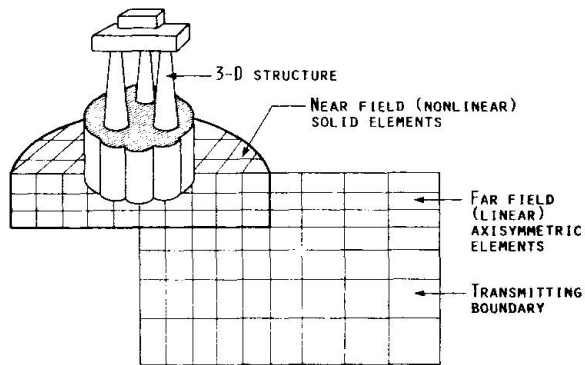


FIG. 10a. Far field-near field modelling

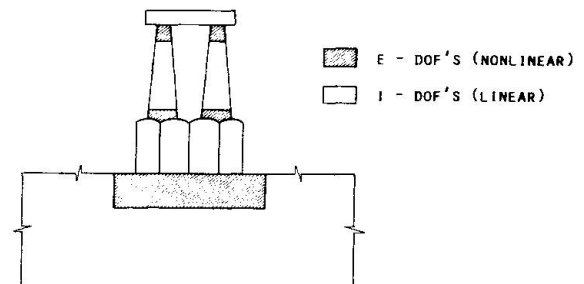


FIG. 10b. Substructuring into linear and nonlinear regions

5. CONCLUSIONS

Design of concrete gravity platforms placed in deep hostile water and in location with very poor soil conditions, calls upon reliable methods and procedures accounting for nonlinearities in the soil, the structure and the soil-structure interaction system. Constitutive models for inelastic behaviour of reinforced concrete have been discussed in connection to their applicability to large-scale nonlinear analysis of deep water gravity platforms. Particular emphasis has been given to a realistic modelling of crack development in concrete. Various computational aspects related to soil-structure interaction have been discussed.

ACKNOWLEDGEMENT

The authors would like to thank Mr. O. Dahlblom, graduate student of Lund Institute of Technology, for carrying out the numerical testing of present concrete cracking model. Our thanks are also extended to other members of the project team of "Integrated Analysis of Gravity Platforms", in particular Dr. G. Svane and Professor T.H. Søreide, for valuable discussions regarding large-scale finite element analysis of concrete offshore platforms.



REFERENCES

1. ERIKSEN K., JAKOBSEN B., MOKSNES J. and SCHETLEIN I.O., The Evolution of the Concrete Structure, Offshore Northern Seas (ONS), Advanced Projects Conference, Stavanger, Norway, 19-21 November 1985.
2. STOKKE K., New Generation Deep Water Structures, Offshore Northern Seas (ONS), Advanced Projects Conference, Stavanger, Norway, 19-21 November 1985
3. EIDE O., Geoteknikk i Nordsjøen ('Geotechnique in the North Sea', in Norwegian), NIF-kurs: Plattformer til havs - samvirke mellom jord og konstruksjon, Trondheim, Norway, 6-8 January 1986.
4. FJUKMOEN Y., Finite Element Analysis of the Condeep Platform A, Block 34/10, Global Analysis, Computas Report 82-6017, 1982, Høvik, Norway.
5. KJEKEN J., NEKSTAD O.J., Gullfaks C, Condeep Type Gravity Platform, Global Analysis, Final Report, Vo. I and II, VERITEC Rep. No. 86-3144, 1986, Høvik, Norway.
6. Målfrid Deepwater Concrete Platform, Veritec Marine Technology Journal, June 1985.
7. BERGAN P.G., NYGÅRD M.K., SANDSMARK N., Technical Needs in Computational Mechanics for the Offshore Oil Industry, Proceedings, Symposium on Future Directions of Computational Mechanics", ASME, Winter Annual Meeting, December 10-11, 1986, Anaheim, California.
8. ARNESEN A., BERGAN P.G and SØRENSEN S.I, Nonlinear Analysis of Reinforced Concrete Structures, Computers and Structures, Vol. 12, pp. 571-579, 1980.
9. BERGAN P.G, FISKVATN A. and SØRENSEN S.I, Nonlinear Analysis and Design of Offshore Structures, ACI-ASCE Symposium on Nonlinear Design of Concrete Structures, Waterloo, Canada, Aug. 1979. Published in Study No. 14, edited by M.Z. Cohn, Solid Mechanics Division, University of Waterloo Press, Waterloo, Ontario, Canada, 1980.
10. FAY C.E, Platform Alternatives for the Troll Field, Proc. of 4th Int. BOSS Conf., Delft, The Netherlands, 1985.
11. LEIJTEN S., Factors Affecting Choice of Design of Foundations of Fixed Platform Concepts for Troll, NIF-kurs: Plattformer til havs - samvirke mellom jord og konstruksjon, Trondheim, Norway, 6-8 January 1986.
12. VAN DER POT B.J.G, The Evolution of the Concrete Structure, Offshore Northern Seas (ONS), Advanced Projects Conference, Stavanger, Norway, 19-21 November 1985.
13. SØREIDE T.H., AMDAHL J. and ARNESEN A., Nonlinear Integrated Soil/Structure Analysis of Gravity Platforms, NIF-kurs: Plattformer til havs - samvirke mellom jord og konstruksjon, Trondheim, Norway, 6-8 January 1986.
14. OTTOSEN N.S, A Failure Criterion for Concrete, Journal of the Engineering Mechanics Division, ASCE, Vol 103, No. EM4, pp 527-535, August 1977
15. WILLAM K.J and WARNKE E.P, Constitutive Model for the Triaxial Behaviour of Concrete, Int. Association of Bridge and Structural Engineers, Seminar on "Concrete Structures Subjected to Triaxial Stresses", Paper III-1, Bergamo, Italy, May 17-19 1974.
16. EIBL J. et al., Concrete under Multiaxial States of Stress - Constitutive Equations for Practical Design, Comite Euro-International du Beton, Bulletin No. 156, June 1983.
17. Constitutive Relations and Failure Theories, Chapter 2 in "Finite Element Analysis of Reinforced Concrete", ASCE, New York, 1982.



18. OTTOSEN N.S., Nonlinear Finite Element Analysis of Concrete Structures, Risø National Laboratory, Roskilde, Denmark, Risø-R-411, May 1980.
19. BERGAN P.G., Some Aspects of Interpolation and Integration in Nonlinear Finite Element Analysis of Concrete Structures, Proc. Int. Conference on Computer Aided Analysis and Design of Concrete Structures, Split, Yugoslavia, Sept. 17-21, 1984, Eds. F. Damjanic et al., Pineridge Press, pp. 301-316, 1984.
20. RASHID Y.R., Ultimate Strength Analysis of Reinforced Concrete Pressure Vessels, Nuclear Engineering and Design, Vol. 7, No. 4, pp 334-344, April 1968.
21. BAZANT Z.P. and CEDOLIN L., Blunt Crack Band Propagation in Finite Element Analysis, Journal of the Engineering Mechanics Division, ASCE, Vol. 105 No. EM2, pp 297-315, April 1979
22. PETERSON P.E., Crack Growth and Development of Fracture Zones in Plain Concrete and Similar Materials, Report TVBM-1006, Div. of Building Materials, Lund Institute of Technology, Sweden, 1981.
23. HILLERBORG A., MODEER M. and PETERSON P.E., Analysis of Crack Formation and Crack Growth in Concrete by Means of Fracture Mechanics and Finite Elements, Cement and Concrete Research, Vol. 6, 1976, pp 773-782.
24. BAZANT Z.P and OH B.H., Crack Band Theory for Fracture of Concrete, Materials and Structures, RILEM, Vol. 16, 1983, pp 155-177.
25. OTTOSEN N.S., Thermodynamical Consequences of Strain Softening in Tension, Jour. of Engineering Mechanics, ASCE, Vol. 112, No EM11, pp 1152-1164, November 1986.
26. OTTOSEN N.S., DAHLBLOM O., Smearred Crack Analysis Using a Nonlinear Fracture Model for Concrete, Proc. at Third Int. Conf. on Num. Meth. for Nonlinear Problems, Dubrovnik, Yugoslavia, September 15-18, 1986.
27. DAHLBLOM O., OTTOSEN N.S., Smearred Crack Analysis Using the Fictitious Crack Model, Submitted to Journal of Engineering Mechanics, ASCE, 1987
28. DAHLBLOM O., Constitutive Modelling and Finite Element Analysis of Concrete Structures Considering Environmental Influence, Div. of Structural Mechanics, Rep. TVSM-1004, Lund Institute of Technology, Sweden 1987
29. HAN D.J. and CHEN W.F., Constitutive Modelling in Analysis of Concrete Structures, Report No. CE-STR-84-19, School of Civil Engineering, Purdue University, Indiana, USA, May 1984.
30. CERVENKA V. and GERSTLE K.H., Inelastic Analysis of Reinforced Concrete Panels: Theory, Int. Association for Bridge and Structural Engineering Publications, Zürich, Switzerland, Vol. 31-II, 1971, pp 31-45.
31. TINGLEFF O., A Method for Simulating Concentrated Forced and Local Reinforcement in Stress Computations, in "The Mathematics of Finite Elements and Applications", Edited by Whitman, J.P., Academic Press, New York, 1973, pp 463-470.
32. KVALSTAD T.J., Effect av usikre last- og jorddata (The effect of uncertain load- and soil data, in Norwegian), NIF-kurs; Platformer til havs - samvirke mellom jord og konstruksjon, 4-8 januar 1986, Trondheim, Norway.
33. WOLF J.P., Dynamic Soil-Structure Interaction, Prentice-Hall Inc., Englewood Cliffs, New Jersey, 1985



34. BAYO E. and WILSON E.L., Numerical Techniques for the Evaluation of Soil-Structure Interaction Effects in the Time Domain, Report No. UCB/EERC-83/04 Earthquake Engineering Research Center, University of California, Berkeley, 1983.
35. CLOUGH R.W. and WILSON E.L., Dynamic Analysis of Large Structural Systems with Local Nonlinearities, Computer Methods in Applied Mechanics and Engineering 17/18, 1979, pp 107-129.

Leere Seite
Blank page
Page vide